THE EUROPEAN
PHYSICAL JOURNAL
SPECIAL TOPICS

Review

Application of the Josephson effect in electrical metrology

B. Jeanneret[1,a] and S.P. Benz[2,b]

[1] Federal Office of Metrology (METAS), Lindenweg 50, 3003 Bern-Wabern, Switzerland
[2] National Institute of Standards and Technology (NIST), Boulder, CO 80305, USA

Abstract. Over the last 30 years, metrology laboratories have used the quantum behavior of the Josephson effect to greatly improve voltage metrology. The following article reviews the history and present status of the research and development for Josephson voltage standards. Specifically, the technology and performance of voltage standards that have quantum accuracy is explained in detail, as is their impact on a wide range of electrical metrology applications, primarily those for dc and ac voltage measurements. The physics of the Josephson effect will be presented and the importance of quantum-based electrical standards will be discussed. A detailed explanation of the operation of the conventional Josephson voltage standard and its use for dc applications will be presented, including a description of the most important results. The latter sections of this paper describe recent efforts to apply the Josephson effect to ac voltage and other electrical metrology applications. Advanced voltage standard systems have been developed that provide new features such as stable, programmable dc voltages and quantum-accurate ac waveform synthesis. The superconducting technology and integrated circuit designs for these systems will be described. Two different systems have dramatically improved precision measurements for audio-frequency voltages and for electric power metrology.

1 Introduction

During the last century, the International System of Units – the SI – has evolved from an artefact based system to a system based mainly on fundamental constants and atomic processes. The modern units have major advantages over their artefact counterparts: they do not depend on any external parameters such as ambient conditions and, most importantly, they do not drift with time. In addition, they can be simultaneously realized in laboratories all over the world, which strongly simplifies and improves the traceability of any measurements to primary standards.

With the discovery of the Josephson and quantum Hall effects, two electrical quantum standards became available. As an important consequence, the world-wide consistency in the representation and maintenance of the electrical units and the electrical measurements based on them has improved a hundredfold in the last decade. The two quantum effects will also certainly play a major role in the next modernization of the SI when the last base unit still based on an artefact, the kilogram, is linked to fundamental constants.

---

[a] e-mail: `blaise.jeanneret@metas.ch`
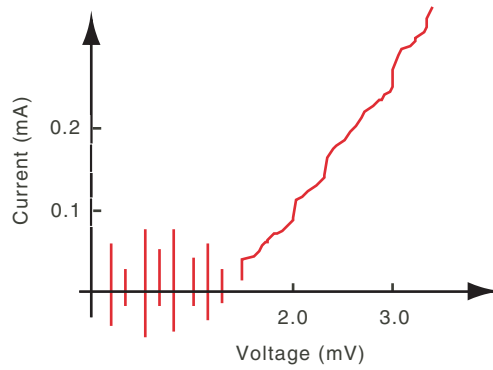[b] e-mail: `benz@boulder.nist.gov`

Fig. 1. Current voltage characteristic of a weakly damped Josephson junction.

In 1962, Brian Josephson published a theoretical study on transport phenomena in weakly coupled superconductors [1]. The prediction of quantized voltage steps in such systems, called Josephson junctions, was experimentally confirmed by Shapiro [2]. When a Josephson junction is exposed to electromagnetic radiation of frequency f, its current-voltage characteristic exhibits precisely quantized voltage steps (see Fig. 1) described by the relation $V_n = nf/K_J$ where n is the step number. K_J is the Josephson constant, which – according to the present theoretical and experimental evidence – is given by:

$$K_J = 2e/h, \tag{1}$$

where e is the elementary charge and h the Planck constant. These Shapiro steps form the basis of the Josephson voltage standard (JVS).

In section 2, the implication of the discoveries of both the Josephson and the quantum Hall effect (QHE) on the system of electrical units is summarized. Although this paper mainly focuses on the application of the Josephson effect, the role of the von Klitzing constant $R_K = h/e^2$ on the representation of the electrical units is also considered for completeness. For the interested reader, a comprehensive review of the application of the quantum Hall effect in metrology can be found in [3]. Section 3 describes in detail both the traditional Josephson voltage standard for dc applications and the newly developed programmable and pulse-driven standards for ac applications.

2 The conventional system of electrical units

The Josephson and quantum Hall effects can be used to realize very reproducible voltage and resistance values, which to our knowledge, depend only on fundamental constants. To be used as practical standards, the value of the Josephson and von Klitzing constants have to be known in SI units. In the SI, the electrical units are defined in terms of the mechanical base units metre, kilogram, and second through the definition of the ampere and the assumption that electrical power and mechanical power are equivalent. To put the concept of the electrical units into practice, it is sufficient to realize two electrical units in terms of the metre, kilogram, and second. At present, the farad and the watt are the two chosen units, since they are the most accurately determined.

2.1 The determination of R_K and K_J

To measure the von Klitzing constant, the quantized Hall resistance (QHR) has to be compared to a resistance standard whose value is known in SI units. In practice, the unit ohm is realized by means of a calculable cross capacitor based on an electrostatics theorem discovered in 1956
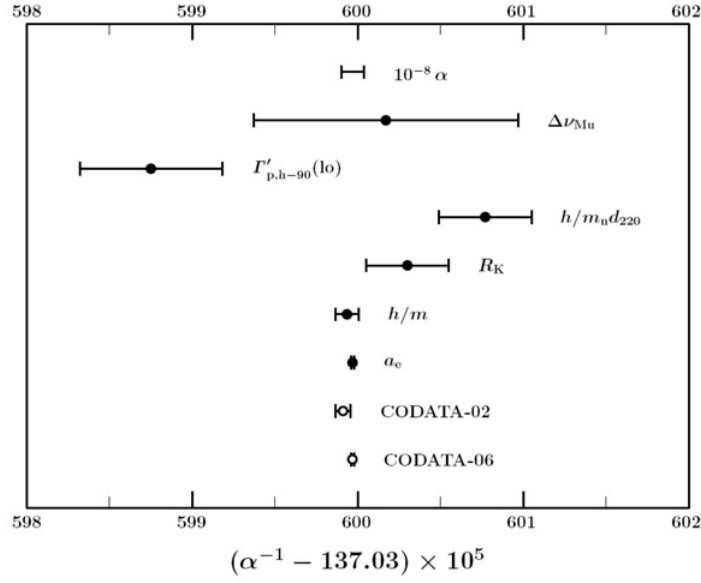
Fig. 2. Values for the fine structure constant taken into account in the 2006 adjustment of the fundamental constants [8]. Γ'_{90} is the value from the measurement of the gyromagnetic ratio of the shielded proton; $\Delta\nu_{Mu}$ is related to the muonium ground-state hyperfine splitting, a_e to the anomalous magnetic moment of the electron. h/m is the ratio of the Planck constant to various atomic masses.

by Thompson and Lampard [4]. When the theorem is correctly put into practice, the cross capacitance depends only on the capacitor length. By use of ac bridge techniques, the capacitance of the calculable capacitor is scaled to a value, which can be compared to the resistance of an ac resistor using a quadrature bridge. After proper scaling, this ac resistor is compared to another ac resistor that has a small and calculable ac/dc difference. Finally, dc techniques are applied to link the calculable resistor to the QHR. Despite the long and complicated measurement chain, an accuracy of a few parts in 10^8 is attainable using this method [5–7].

There is an important consequence of the QHE in the field of fundamental constants, which should also be addressed here. The von Klitzing constant R_K is related to the fine structure constant through the simple relation

$$R_K = \frac{h}{e^2} = \frac{\mu_0 c}{2\alpha}. \tag{2}$$

In the SI, the permeability of vacuum μ_0 and the speed of light c are fixed quantities with $\mu_0 = 4\pi \times 10^{-7}\,\mathrm{N\,A^{-2}}$ and $c = 299\,792\,458\,\mathrm{m\,s^{-1}}$. The fine structure constant can thus be used to determine R_K and test possible corrections to the QHR. Conversely, if R_K is assumed to be identical to the QHR, the QHE opens up an additional route to the determination of α that does not depend on QED calculations. In Fig. 2, all the results are shown that contributed to the least square adjustment of α, as given in the 2006 set of fundamental physical constants recommended by the CODATA task group [8].

At present, the most accurate value for α is derived from the anomalous magnetic moment a_e of the electron measured by use of single electrons or positrons stored in a Penning trap at 4.2 K and exposed to a magnetic flux [9]. A relative experimental uncertainty of 6.9×10^{-10} has been reached so far [8]. A value for the fine structure constant can be obtained from the experimental value of a_e by comparing it to the theoretical value, which can be, up to some insignificant correction terms due to electroweak and hadronic interactions, expressed in the framework of quantum electrodynamics as a power series in α. The most important terms in the series can be calculated analytically, but for some of the higher-order terms extensive numerical calculations are necessary [10].

The second most important result taken into account in the calculation of the actual value for α comes from the realization of R_{K} through the calculable capacitor assuming that the QHR is equal to R_{K}. As the comparison shows, R_{K} and the a_e derived value for α agree only fairly within the experimental uncertainty.

The Josephson constant K_{J} can be determined by comparing the Josephson voltage to a voltage standard known in terms of the SI unit volt. The volt can be realized directly in an electromechanical experiment where an electrostatic force arising from a voltage is counterbalanced with a known gravitational force. The accuracy of these experiments (see [8] for a review) is limited to approximately $0.6\,\mu\mathrm{V/V}$.

A more accurate route to K_{J} is the watt balance experiment [11] in which electrical and mechanical power are compared. If the electrical power is measured in terms of the Josephson voltage and the quantized Hall resistance, then the product $K_{\mathrm{J}}^2 R_{\mathrm{K}}$ is determined in the experiment. The most accurate result so far was obtained at the National Institute of Standards and Technology (NIST) [12] with an uncertainty of 4 parts in 10^8 for the product $K_{\mathrm{J}}^2 R_{\mathrm{K}}$.

2.2 Conventional values for R_{K} and K_{J}

The best realizations of the volt and the ohm in the SI are about two orders of magnitude less accurate than the reproducibility of quantum standards based on the Josephson and the quantum Hall effects. Two electrical units realized in terms of the non-electrical SI units metre, kilogram, and second are needed to make the other electrical units measurable in the SI. With the QHE and the Josephson effect, two fundamentally stable standards are available and thus it was realized that the world-wide consistency of electrical measurements could be improved by defining conventional values for R_{K} and K_{J}. The Comité Consultatif d'Électricité (CCE) was asked to recommend such values based on the data available. All the values for R_{K} and K_{J} available by June 1988 in SI units were analysed and the following conventional values were proposed [13]:

$$R_{\mathrm{K\text{-}90}} = 25812.807 \ \Omega$$
$$K_{\mathrm{J\text{-}90}} = 483597.9 \ \mathrm{GHz/V}.$$

Relative uncertainties with respect to the SI of 2×10^{-7} and 4×10^{-7}, respectively, were assigned to the two values. The conventional values were accepted by all member states of the Metre Convention and became effective as of January 1, 1990. Due to further experimental progress, the assigned uncertainty for R_{K} with respect to the ohm was reduced in 2000 by a factor of two to 1×10^{-7}.

In the case of $R_{\mathrm{K\text{-}90}}$, the value chosen was essentially the mean of the most accurate direct measurements of R_{K} based on the calculable capacitor and the value from the calculation of the fine-structure constant based on the anomalous magnetic moment of the electron [13]. In the most recent least-square adjustment of fundamental constants carried out by the CODATA Task Group on Fundamental Constants [8], a value of $R_{\mathrm{K}} = 25812.807557 \ \Omega$ with a relative uncertainty of 6.8 parts in 10^{10} was evaluated. This new value is in good agreement with the conventional value, $R_{\mathrm{K\text{-}90}}$. Figure 2 shows the results that were taken into account in the calculation of the new R_{K} value and consequently the new recommended value for α.

In the case of $K_{\mathrm{J\text{-}90}}$, the value chosen was dominated by the watt balance result obtained at the National Physical Laboratory (NPL) [14] and the value of R_{K}. In the CODATA 2006 adjustment, a value of $K_{\mathrm{J}} = 483597.891 \ \mathrm{GHz/V}$ with a relative uncertainty of 2.5 parts in 10^8 was evaluated. Again, this is in a very good agreement with the conventional value $K_{\mathrm{J\text{-}90}}$.

3 The Josephson voltage standard

Development of the Josephson array voltage standard started with the discovery of the Josephson effect in 1962. Nowadays, numerous Josephson voltage standards are in use around

the world in national, industrial, and military standard laboratories. These standards can reach a voltage of 10 V with an uncertainty that is typically smaller than 1 part in 10^9. The development, design, and operation of the Josephson voltage standard has been the subject of many detailed review papers [15–22]. The present section is rather a short and basic introduction to the subject, and includes new developments related to the application of the Josephson effect in ac voltage metrology.

3.1 Theoretical background of the Josephson effect

In 1962, Josephson [1] predicted several effects associated with the tunnelling of Cooper pairs in a junction consisting of two superconducting electrodes separated by a thin insulating barrier. In particular, when such an ideal junction is connected to an external source, the current flow through the junction is described by the two equations:

$$I = I_c \sin \varphi \tag{3}$$

$$V = \frac{\hbar}{2e} \frac{d\varphi}{dt} = \frac{h}{2e} f_J, \tag{4}$$

where φ denotes the phase difference between the two macroscopic wave functions of the superconducting electrodes, I_c is the critical current of the junction and $\hbar = h/2\pi$. The first equation (dc Josephson effect) implies that a current can flow without a dc voltage across the junction as long as the current is smaller than the critical current. If the critical current is exceeded, a voltage appears across the junction, which gives rise to an alternating current of frequency f_J (ac Josephson effect). Conversely, irradiation of the junction with microwaves of frequency f produces steps of constant voltage V_n due to the phase locking of the Josephson oscillator to the external frequency:

$$V_n = n \frac{h}{2e} f, \tag{5}$$

where n is the step number. These voltage steps, which were observed for the first time in 1963 by Shapiro [2], form the basis of the quantum voltage standard.

In a real Josephson junction, the ideal junction is always shunted by its own capacitance C and resistance R. The dynamics of such a junction is often investigated by the so called resistively and capacitively shunted junction (RCSJ) model [23,24]. The second Josephson equation is modified to take into account the current flow in the resistance and the capacitance. The equation describing the circuit when the junction is biased by both a dc current I_0 and an ac current I_{rf} of frequency $f = \omega/2\pi$ is

$$\frac{\hbar C}{2e} \frac{d^2\varphi}{dt^2} + \frac{\hbar}{2eR} \frac{d\varphi}{dt} + I_c \sin \varphi = I_0 + I_{rf} \sin(\omega t). \tag{6}$$

This model properly describes the behaviour of the junction when the current is uniformly distributed over the junction area: $I_c = wlJ_c$, where w is the junction width, l is the junction length (both perpendicular to the direction of the current through the barrier) and J_c is the critical current density. The dynamics of the junction is thus described by a strongly non-linear second-order differential equation. Such non-linear systems are prone to show chaotic behaviour (see [25] for a review), which must be avoided for metrological applications by a careful optimization of the junction parameters.

For small phase difference, Eq. (4) becomes $V = (\hbar/2eI_c)dI/dt = L_J dI/dt$, where $L_J = \hbar/2eI_c$ is the kinetic inductance of the junction. In this case, the Stewart-McCumber model is an LCR resonator circuit with a resonance frequency $\omega_p = (L_J C)^{1/2} = (2eI_c/\hbar C)^{1/2}$ called the plasma frequency. A fundamental parameter of the junction is the McCumber damping parameter β_c defined as the square of the quality factor of the LCR resonator $Q = R(C/L)^{1/2}$:

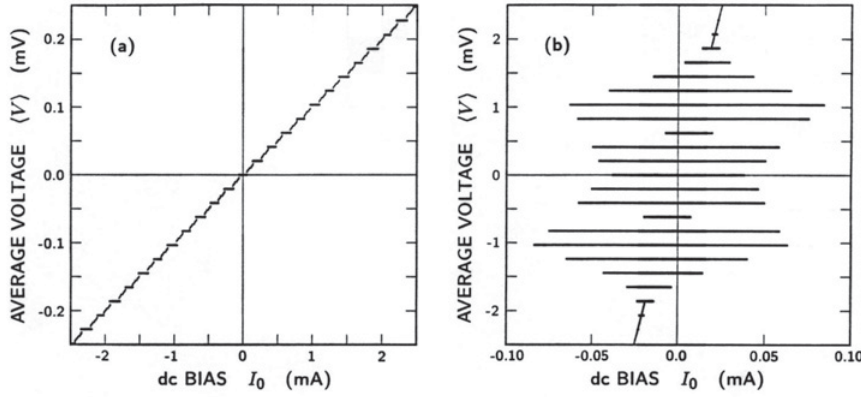$$\beta_c = \frac{2e}{\hbar} I_c R^2 C. \tag{7}$$

Fig. 3. Simulated current-voltage curve computed by use of the Stewart-McCumber model in the limit (a) $\beta_c \leq 1$ and (b) $\beta_c \gg 1$ (after [25]).

In the limit $\beta_c \gg 1$, the junction is underdamped and shows a hysteretic IV curve (see Fig. 3b); such junctions are used in conventional Josephson voltage standards. In the opposite limit $\beta_c \leq 1$, the junction is overdamped and its IV curve is single-valued (see Fig. 3a); such junctions are at the heart of the newly developed programmable Josephson voltage standards (PJVS).

When the junction is phase-locked to the microwave current, the supercurrent is forced to oscillate at the frequency f (or any of its higher harmonics nf). This synchronization of the junction to the external current generates voltage steps V_n (given by Eq. (5)) in the IV curve. These steps occur over a range of dc current ΔI_n (step width) given by the nth-order Bessel function J_n:

$$\Delta I_n = 2I_c |J_n(2eV_{rf}/hf)|, \tag{8}$$

where V_{rf} denotes the amplitude of the radio-frequency voltage across the junction.

3.2 Universality tests

The accuracy of the voltage-frequency relation was tested in different types of junctions and arrays [26–30]. These highly precise and accurate experiments were based on a method using a superconducting quantum interference device (SQUID) magnetometer [31] as depicted in Fig. 4. The junctions (or the arrays) to be compared are mounted in series opposition. The superconducting loop includes the two Josephson devices, the SQUID input inductance L_s and the two parasitic inductances L_1 and L_2, which are combined to yield the total loop inductance $L = L_s + L_1 + L_2$. Each device must be biased on the same voltage step using the bias supply I_1 and I_2. The microwave power is supplied to both devices by the same Gunn diode to avoid any effect coming from small frequency variations.

Once the two Josephson devices have been biased on the appropriate voltage step, the switch can be closed. Any voltage difference will lead to a superconducting current I_s increasing linearly in time, which can be very sensitively detected by the SQUID. This current is given by

$$I_s = \frac{1}{L} \int (V_1 - V_2) dt, \tag{9}$$

where V_1 and V_2 are the Josephson voltages.

In 1983, this experiment was performed to compare a Nb-Cu-Nb junction to an In microbridge [26]. Although the two junctions are of a very different nature (material, geometry, etc...), no voltage difference was observed to 2 parts in 10^{16}. This method was later used to measure the resistive slope of a voltage step at a voltage of 1 V [27]. Over the $20\,\mu$A width of a quantized step at 1 V, the variation of the step voltage was smaller than 7 parts in 10^{13}. In 1987, the
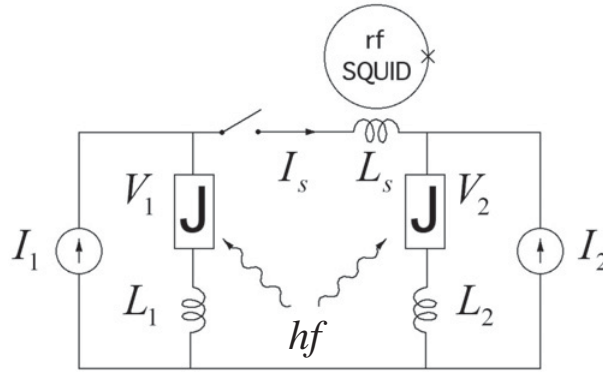
Fig. 4. Principle of a high-accuracy comparison between two Josephson junctions or arrays (after [29]).

effect of the gravitational field on charged particles was tested by measuring the voltage difference between two similar single junctions vertically separated by a distance of 7.2 cm [28]. No voltage difference was measured to 3 parts in 10^{19}, in agreement with the predicted invariance of the gravito-electrochemical potential. Josephson junction arrays were also tested using this method. In 1987, it was shown that two arrays made of Nb/NbO/PbInAu junctions differed in voltage by less than 2 parts in 10^{17} at 1 V. This experiment was repeated later with two arrays made of Nb/Al/AlO$_x$/Al/AlO$_x$/Al/Nb junctions [30]. No voltage difference was observed to 2 parts in 10^{17}.

Although these experiments do not prove that the Josephson constant K_J is really $2e/h$, they give convincing experimental evidence that K_J is a universal quantity with no known corrections to the ac Josephson voltage equation. The major result of these experiments was nicely summarized by P.W. Anderson: «... it shows that gauge invariance is exact.» [32].

3.3 Conventional Josephson voltage standard

In the 1970's, the voltage standard consisted of single junctions, which provided only small voltages, typically 5 mV to 10 mV. Although the stability of the single-junction standard already exceeded the stability of the primary Weston cell standard, comparing the Weston cell to the Josephson standard required a precise voltage divider that was difficult to calibrate with the required accuracy. Therefore, attempts were made to increase the Josephson voltage output by connecting several junctions in series. The most ambitious project [33] used 20 junctions in series to produce a voltage of 100 mV with an uncertainty of a few parts in 10^9. Twenty individually adjustable current sources were needed to ensure that each junction remained on the appropriate voltage step. The difficulty of the tuning procedure prevented this approach from being widely implemented.

The multiple bias problem was solved using a suggestion made by Levinsen [34] in 1977. Levinsen showed that a highly capacitive junction with a large McCumber parameter ($\beta_c > 100$) can generate an hysteretic IV curve with voltage steps that cross the zero-current axis, hence their name of zero-crossing steps (see fig. 3b). The lack of stable regions between the first few steps shows that the voltage of the junction must be quantized, at least for small current bias.

After the problems of junction stability and microwave power distribution were solved, the first large array based on the Levinsen idea was fabricated [35], leading to the first practical 1 V Josephson voltage standard (JVS) in 1985 [36,37]. Improvements in the superconductive integrated-circuit technology allowed the fabrication of the first 10 V array in 1987 [38]. This array consisted of 14'484 junctions that generated about 150'000 quantized voltage steps spanning the range between -10 V and 10 V. The 10 V JVS was then implemented in many National Metrology Institutes (NMI). The accuracy of these standards is determined by international comparisons between the transportable Josephson system of the Bureau International des Poids et Mesures (BIPM) and those of the NMI. Typically, the difference between two quantum
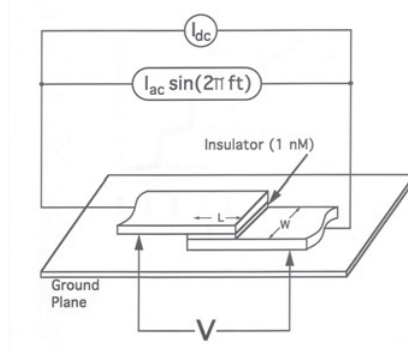
Fig. 5. Schematic of a typical SIS junction used in an large array (after [19]).

standards is less than 1 part in 10^9 at a voltage of 10 V. The best comparisons, however, have uncertainties on the order of a few parts in 10^{11} [39].

In the next paragraphs, the conventional JVS will be described in more detail.

3.3.1 Junctions and array designs

Nowadays, all the SIS junctions for conventional JVS systems for application in voltage metrology are fabricated with planar $Nb/Al_2O_3/Nb$ thin-film structures (see Fig. 5). Developed during the 1980's, this technology has several advantages:

- Sputtering of the thin-film sandwich that forms all the junctions can be performed without breaking the vacuum. This ensures very clean interfaces and allows oxidation of an extremely thin and homogeneous insulating junction barrier.
- Using Nb, the junctions are mechanically and chemically stable. This was not the case with the lead-alloy junctions used earlier. As a result, no aging of the Josephson arrays is observed.
- Since the critical temperature of Nb is 9 K, the circuit can be operated in liquid He at a temperature of 4.2 K. At a temperature of half the critical temperature, all the superconducting parameters have approached their $T = 0$ value.

The most important condition for accurate measurements using a conventional JVS is the stability of the phase lock between the microwave current and the Josephson oscillator. This phase lock must be strong enough to prevent the array from frequently jumping from one voltage step to another during the course of a calibration. On the basis of the McCumber model, Kautz analyzed how the various junction parameters influence the stability of the phase lock with regard to chaos, thermal noise and uniformity of the current distribution (see [16,25] for a review). Four conditions are required for stable operation of the conventional standard:

1. The junction length l must be small enough that the flux created by the microwave current over the junction's surface is much less than the flux quantum $\phi_0 = h/2e$.
2. Both the junction width w and length l must be small enough that the lowest resonant cavity mode of the junction is greater than f.
3. To avoid chaotic behaviour, the plasma frequency must satisfy the relation $f_p < f/3$. Since $f_p \propto J_c^{0.5}$, the critical current density is limited to $J_{cmax} = (f/3)^2(\pi h C_s/e)$, where C_s is the specific capacitance of the junction $C_s = C/wl$. Together with the limitation of the first and second condition, the critical current is therefore limited to $I_{cmax} = w_{max}l_{max}J_{cmax}$, which in turn limits the maximum step width to $\Delta I_{nmax} = 2I_{cmax}|J_n(2eV_{rf}/hf)|_{max}$.
4. The critical current should be as large as possible to prevent noise-induced step transitions; in other words, the coupling energy of the junction $E_J = \hbar I_c/2e$ must be larger than the thermal fluctuations kT.

Conditions three and four are clearly antinomic. Therefore, the stability of the array is caught in a region of the parameter space between instabilities due to thermal noise or chaos. However, an optimized design can lead to excellent stability that is sufficient for most dc calibrations. As an example, the set of parameters given in Table 1 for a typical 10 V array ensures stability of several hours under appropriate conditions.

Table 1. Junction design parameters (after [19]).

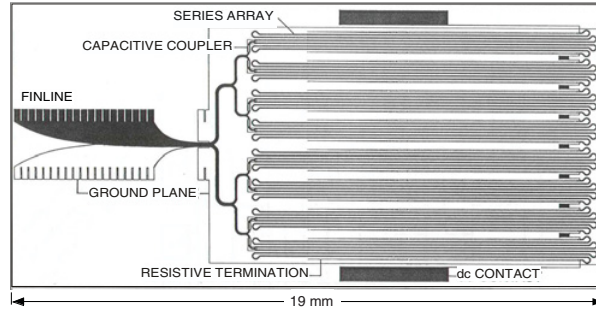| Junction material	Nb/Al$_2$O$_3$
Critical current density J_c	$20\,\text{A/cm}^2$
Junction length l	$18\,\mu\text{m}$
Junction width w	$30\,\mu\text{m}$
Critical current I_c	$110\,\mu\text{A}$
Plasma frequency f_p	$20\,\text{GHz}$
Lowest resonant cavity mode	$175\,\text{GHz}$
Microwave frequency f	$75\,\text{GHz}$
Specific capacitance C_s	$5\,\mu\text{F/cm}^2$

Fig. 6. Schema of a typical 10V NIST array (after [19]). This design is the result of a joint NIST/PTB effort (see [18,21,35]).

For this 10 V array design, 20'208 junctions form a series array, as shown in the schematic of Fig. 6. The microwave power is collected by a finline antenna, split 16 ways, and injected into 16 segments, each containing 1263 junctions distributed along the micro-stripline. The most important consideration in the design of the array is that each junction must receive the same microwave power in order to develop the largest possible zero-crossing steps. The maximum number of junctions per segment is limited by the attenuation of the stripline. Microwave reflection at the end of each stripline is suppressed by a distributed lossy load. To meet the appropriate packaging density, the striplines are folded, taking into account that the microwave bend radius has a minimum value of three times the stripline width. All the segments are connected in series to produce the maximum dc voltage. The dc voltage is measured across superconducting pads placed at the edge of the chip via low pass filters.

3.3.2 Measurement system

A block diagram of a typical conventional JVS is shown in Fig. 7 (after [21]). The array is mounted in a magnetically shielded cryoprobe fitted with a WR-12 waveguide and three pairs of heavily filtered wires. The cryoprobe is immersed in liquid helium at 4.2 K. The microwave power is provided by a Gunn diode, which operates at a frequency range of 70 to 90 GHz. The Gunn must have enough power to deliver around 15 mW at the chip finline for a 10 V array. An attenuator allows adjustment of the power to the array, and a directional coupler diverts
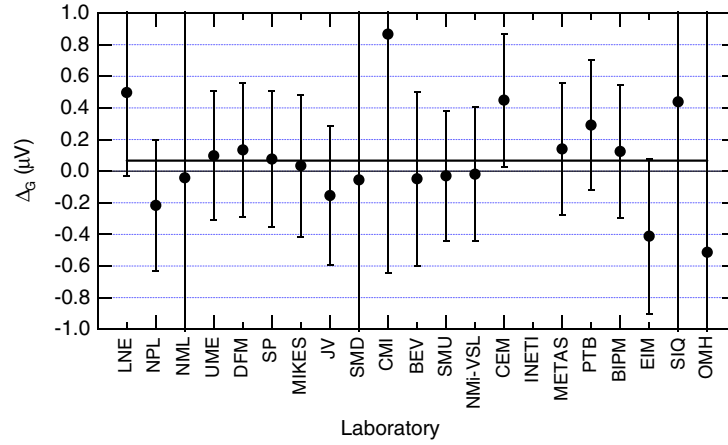
Fig. 7. Block diagram of a typical Josephson voltage standard (after [21]).

part of the power to the phase-locking counter, which establishes the phase lock to the external frequency reference (most of the time a Cs clock or a GPS receiver).

A low-frequency triangle-wave generator is used to trace the IV curve of the array on the oscilloscope's screen. This allows measurement of the critical current, the IV curve, and the constant-voltage steps in order to optimize the power settings and to maximize the width of the zero-crossing steps. Tuning the power is the most critical parameter adjustment (see [15] on how to proceed). A voltage source connected to the array through a variable resistor allows selection and stabilization of the desired voltage step.

The device under test (DUT) is connected to one pair of wires, most of the time through a switch or a scanner, which allows reversal of the polarity of the DUT and measurement of the voltage difference between the array and the DUT with a null-detector.

Although the voltage appearing at the Josephson array is, in principle, exact; the accuracy of the precision voltage measurement is limited by a large number of uncertainties. A list of all the identified sources of uncertainty is given below:

1. Reference frequency offset and noise
2. Leakage current in the measurement loop
3. Detector gain error
4. Detector bias current
5. Nanovoltmeter offset, input impedance, nonlinearity and noise
6. Uncorrected thermal voltages
7. Rectification of the reference frequency current
8. Electromagnetic interference
9. Sloped steps (bias-dependent voltages)

In the above list, only uncertainties 1 and 2 depend on the voltage being measured. This observation allowed Hamilton to develop a powerful method to collectively evaluate uncertainties 3 to 8 by using a sequence of short circuit measurements [40]. Therefore, the final uncertainty budget of the Josephson voltage standard has only three components. For the 10 V METAS system, using a HP3458A DVM as the null detector, the uncertainty components have the following typical values: 0.7 nV for the frequency, 1.0 nV for the leakage current and 5.0 nV for the repeatability (uncertainties 3 to 8). The combined standard uncertainty of the system is thus 5.1 parts in 10^{10}. This uncertainty can be further reduced to a few parts in 10^{11} mainly by use of an analog nanovoltmeter [39].

Fig. 8. Result of the EUROMET 429 comparison. Δ_G is the value given by each participant – relative to 10 V – for a group of four Zener standards. The solid line is the reference value. See the BIPM database for more details (Ref: EUROMET.EM.BIPM-K11).

3.3.3 Application in dc voltage metrology

The most important application of the conventional Josephson voltage standard is the calibration of Zener-diode-based dc reference standards. Zener standards are convenient transportable voltage standards that are used to maintain the traceability chain to the primary Josephson standard [41] at 1.018 V and 10 V. The stability of the 10 V output of a Zener is around 10^{-6} per year. By carefully controlling the environmental conditions and by modelling temporal drift, output voltages can be predictable over periods of several weeks to within a few parts in 10^8. Ultimately, the uncertainty of the output voltage of a Zener standard is limited by a $1/f$ noise floor having a value between two and ten parts in 10^9 [42,43]. Nevertheless, by using great care, standard uncertainties on the order of a few parts in 10^8 have been achieved by using Zeners as travelling standards in international comparisons (see [44,45] and references therein). As an example, the results of an EUROMET comparison are presented in Fig. 8. EUROMET stands for European Collaboration in Measurement Standards and is the European metrology organization. A group of four Zener standards carefully characterized by the BIPM was sent to the participants. The data represent the result given by each participant for the mean value of the group. The overall agreement is excellent, since most of the results agree within the comparison uncertainty.

Another important application of the conventional Josephson voltage standard is the calibration and linearity measurement of high precision digital voltmeters. An example of such a measurement is given in Fig. 9a. A HP3458A DVM was used to read the output voltage of the Josephson standard for voltages ranging between -10 V and 10 V in steps of 1 V. The gain of this instrument exceeds one by 0.9×10^{-6}. The linearity of the instrument, which is given by the standard deviation of residuals from the fit, is shown in Fig. 9b. The linearity is 350 nV, or in relative units 3.5×10^{-8}, which is outstanding. During the development of this instrument, a Josephson voltage standard was used to characterize the linearity of the analog to digital converters. Clearly, such a linearity would have been impossible to achieve without the use of a Josephson voltage standard [46] in the development phase of the instrument.

3.4 Programmable voltage standards

As described in the previous section, the conventional Josephson voltage standard has enabled metrology laboratories to exploit the quantum behavior of the Josephson effect to greatly improve the accuracy of dc voltage measurements. This section describes two entirely different Josephson voltage standards, which provide new features for a wider range of voltage metrology
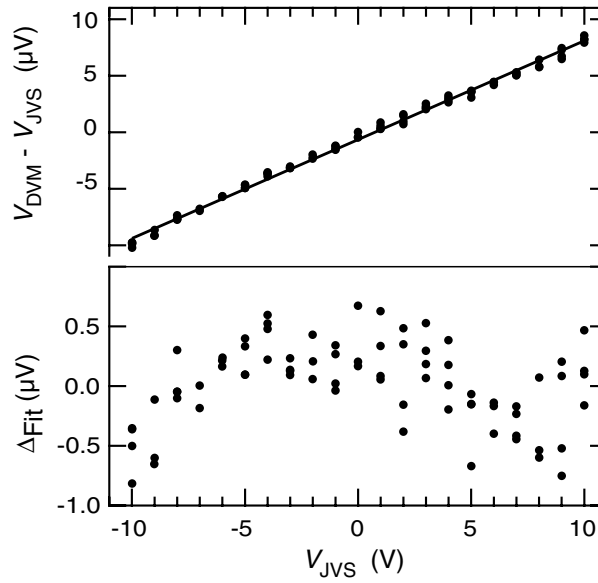
Fig. 9. Measurement of the linearity of a commercial high resolution DMM (HP 3458) in its 10 V range. Data taken at the Swiss Federal Office of Metrology (METAS).

applications that require either stable, programmable dc voltages or ac voltage waveforms with calculable rms voltage. These features are not possible with the conventional JVS because the zero-crossing steps of the SIS Josephson junctions are inherently metastable; this very feature, which enabled large voltages to be produced with arrays of non-identical junctions, prevents their use in these other applications because one cannot predetermine the exact Shapiro step number for any given Josephson junction in an array. Since the quantum state of individual SIS junctions cannot be precisely controlled for an indefinitely long period, the arrays of such junctions also cannot be rapidly and reliably switched between different target voltages, and their application is limited to dc calibration.

Fortunately, significant improvements have been made in both the materials and fabrication techniques of Josephson junctions so that uniform arrays of damped, non-hysteric junctions ($\beta_c < 1$) can now be produced. Single-valued and intrinsically stable electrical characteristics were originally achieved with SIS junctions by externally shunting them with thin-film resistors. The most common method today for producing stable junctions for voltage standards is to fabricate intrinsically shunted junctions by use of a normal metal in the junction barrier, as in Superconductor-Normal metal-Superconductor (SNS) or Superconductor-Insulator-Normal metal-Insulator-Superconductor (SINIS) junctions [47–50].

Improvements in the uniformity of such junctions were critical for developing new Josephson systems and measurement techniques for ac voltage metrology applications. Two systems were developed that exploit the Josephson effect very differently and will be described below: the programmable Josephson voltage standard (PJVS) and the pulse-driven ac Josephson voltage standard (ACJVS). The PJVS system is a superconducting multibit digital-to-analog converter (DAC) that can produce selectable, stable, dc voltages or step-wise approximated waveforms whose accuracy is enhanced because the steps are defined by quantum-accurate constant-voltages [51]. Both the rms accuracy and output frequency of this approach, however, are limited, because the transition time between steps is finite and biasing and timing errors affect the time spent on the voltage steps. The PJVS system is presently used in applications that required rapidly programmable, stable, constant voltages [12,52–54] and for low-frequency applications, such as power metrology at 50 to 60 Hz [55,56].

The second quantum-based ac voltage source is the pulse-driven ACJVS system [57,58]. ACJVS synthesized voltages have quantum accuracy and do not suffer from transient and timing problems like those for the PJVS because the waveforms are produced by controlling every

quantized voltage pulse produced by each junction. Periodic streams of pulses, synchronized to a microwave frequency, bias the arrays of junctions. The arrays behave as perfect pulse quantizers because the time integral of each junction's voltage pulse is quantized in units of $h/2e$, as in the second Josephson relation. Arbitrary voltage waveforms can therefore be generated, and their voltages are accurate and predictable. The ACJVS is sometimes called the Josephson arbitrary waveform synthesizer (JAWS) because of its ability to synthesize low-distortion arbitrary waveforms. ACJVS systems are used primarily for audio-frequency applications, especially for calibration of thermal voltage converters. In the following sections, the operation, system design, and primary features and applications of the two different ac voltage synthesis techniques (PJVS and ACJVS/JAWS) will be described in more detail.

3.4.1 Programmable Josephson voltage standard

For applications that require stable and rapidly programmable dc voltages, Hamilton et al. proposed and developed a new type of Josephson voltage standard [51]. The output voltage $V = nMf/K_J$ of this PJVS system is defined by dividing a series array of M total junctions into smaller independently biased programmable segments and then digitally programming the junction step number n for the junctions in each segment. This multi-bit digital-to-analog converter was originally demonstrated with an array of 2048 SIS junctions that were each externally shunted by $1\,\Omega$ resistors. The array was divided in a binary sequence, as shown in Fig. 10, so that each array segment was independently current biased ($-I_s$, 0, or $+I_s$) at one of three quantized voltages, $n = -1$, 0, or $+1$. The combined total step number for the whole array can thus be set to any integer value between $-M$ and $+M$, where M is the total number of junctions in the array.
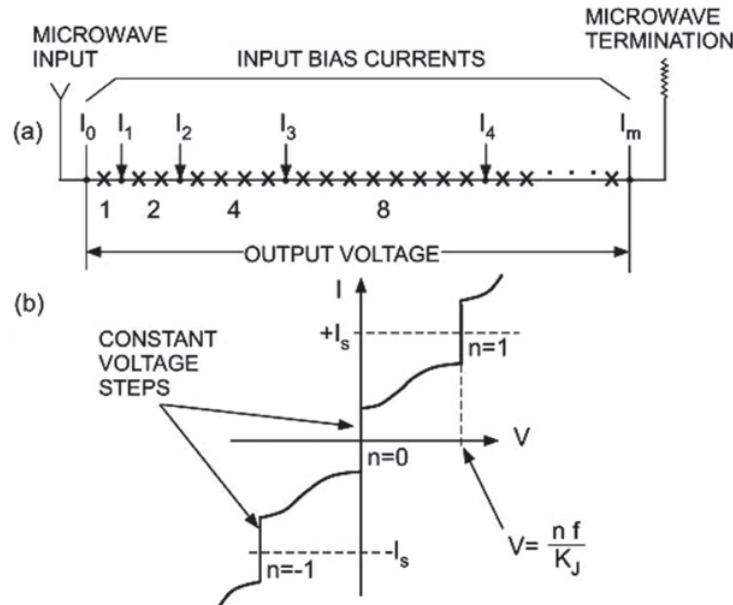

Fig. 10. (a) Schematic design of a programmable voltage standard based on a binary divided array. (b) The IV curve of a single junction with the microwave power set to equalize the current range of each of the $n = \{-1, 0, \text{and} +1\}$ steps (after [19]).

In developing a programmable Josephson voltage standard, the most important characteristics of the Josephson array are stability and fast selection of the desired voltage. Large arrays with sufficient uniformity have been produced with both SNS and SINIS junctions. The high

1 to 10 mA critical currents typical of SNS junctions provide greater immunity to thermal and electrical noise. The low characteristic voltage $V_c = I_c R$ leads to lower operating frequencies (typically $f < 20$ GHz), which is an advantage for the cost of the microwave electronics, but requires four-times as many junctions to achieve the same voltage as SINIS-junctions that typically operate at frequencies around 70 GHz.

In 1997, a 1 V SNS PJVS [59] was demonstrated that used 2 μm $\times$ 2 μm Nb-PdAu-Nb junctions [47] having critical currents $I_c \approx 8$ mA and resistances $R \approx 3$ mΩ, giving characteristic voltages $V_c \approx 24\,\mu$V. The binary-divided array consisted of 32 768 junctions divided into eight arrays, with 4096 junctions each, which were ac-coupled in parallel for the microwave bias and connected in series to produce the maximum dc output voltage (as shown in Fig. 10(a)). One of the arrays was divided into five sub-arrays with 128, 128, 256, 512, 1024, 2048 junctions. The circuit contained a total of 13 series-connected array segments, where the two identical least-significant bit (LSB) segments had 128 junctions each. When a 16 GHz microwave signal was applied and each segment was biased on the $n = 1$ step (with a bias current $I_S \approx 15$ mA), the maximum 1.08 V output was produced. The current range of the steps was typically between 1 mA and 4 mA. Therefore, by selecting the appropriate microwave frequency, number of junctions, and bias currents, it was possible to generate voltages in the range from -1.1 V to $+1.1$ V. The time necessary to transition to a different voltage was limited by the switching time of the bias electronics and by properties of the cryoprobe transmission lines. The accuracy of such a programmable array was checked by comparing the voltages with a conventional Josephson voltage standard [60]. Agreement between the two systems at 1 V was $(1.4 \pm 3.5) \times 10^{-10}$, which was also confirmed in later experiments [61].
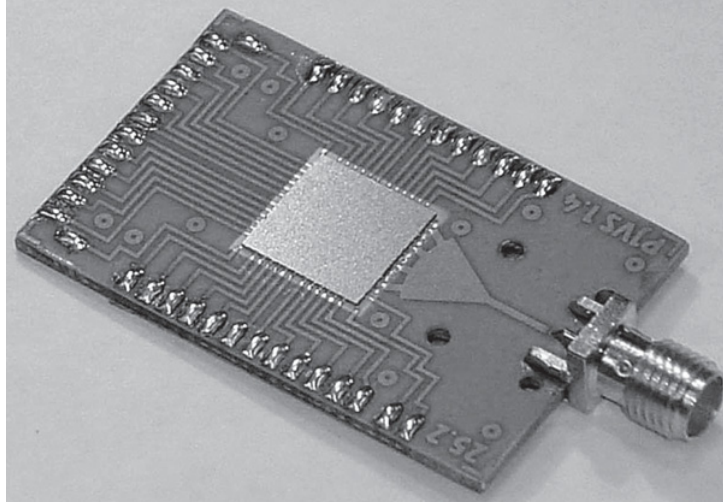

Fig. 11. Photograph of the NIST "flip-chip on flex" cryopackage showing the SMA connector for microwave bias, the on-flex four-way microstrip splitter, and the 40 breakout wiring pads for attaching copper wires for dc biases (courtesy of C.J. Burroughs, NIST, 2005).

The primary goal in improving PJVS performance has been to increase the output voltage to 10 V, so that the PJVS systems can be used for calibrating the maximum voltage of Zener references. NIST has focused on making stacked junctions to increase the output voltage and has successfully developed and applied silicide-based junction barriers. The first successful Nb-based stacked arrays were based on Nb-MoSi$_2$-Nb junctions [62–64]. Double- and triple-stacked arrays of junctions with MoSi$_2$-barriers have delivered voltages up to 3.9 V [64]. NIST also implemented a high-resolution ternary design, which optimally utilizes all three voltage steps, and increases by 16-fold the voltage resolution of the least significant bits (8 junctions (or stacks) vs. 128 junctions) [63]. To improve connection reliability, NIST developed a flip-chip-on-flex cryopackage (see Fig. 11) that allowed a portion of the microwave divider circuits
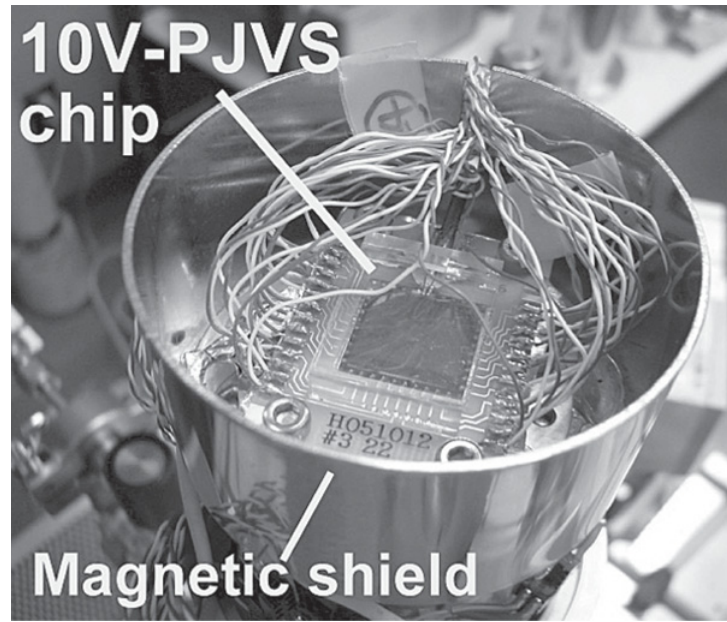
Fig. 12. Photograph of an AIST niobium-nitride based 10 V PJVS chip that is mounted on a cryocooler. (courtesy of A. Shoji and H. Yamamori, AIST, 2007).

to be moved off-chip [65]. More recent NIST circuits have used amorphous niobium-silicide (a-Nb_xSi_{1-x}) barriers and advanced microwave designs, such as tapered transmission lines, to increase the output voltage to 5.2 V with 132,000 total junctions (divided equally into 8 parallel arrays) biased at 20 GHz [66,67]. Maximizing the voltage per array is important for optimizing the efficiency of PJVS circuits because fewer parallel microwave-biased arrays require smaller microwave input power and produce less on-chip dissipation, which in turn reduces cooling requirements. NIST is currently designing 10 V PJVS circuits with only 8 and 16 parallel microwave-biased arrays.

Other research groups have also made important performance improvements for PJVS systems and have explored different approaches to realize 10 V output voltages. Researchers at the National Institute of Advanced Industrial Science and Technology (AIST) developed the first stacked-junction arrays based on NbN superconductors, which can operate at higher (10 K) temperatures that are more easily, and affordably, reached with cryocooler technology. Their junction technology used titanium-nitride barriers and double-junction stacks with the following composition: $NbN/TiN_x/NbN/TiN_x/NbN$. They demonstrated 1 V array circuits in 2005 [68,69] with this technology. Further improvements in circuit design and junction uniformity lead to 10 V chips with 307,200 junctions in 32 parallel arrays that operated at a temperature of 10.2 K with a current range larger than 1 mA [70,71]. Figure 12 shows a photograph of an AIST 10 V chip mounted on a chip carrier in a cryocooler. In order to guarantee 10 V operation, AIST is currently integrating two of their chips in series because perfect operation of all junctions is still a challenge for this technology.

Researchers at the Physikalisch-Technische Bundesanstalt (PTB) have focused their PJVS circuit development efforts on SINIS junctions, which consist of a multilayer of $Nb/Al/AlO_x/Al/AlO_x/Al/Nb$ [49,72]. Such junctions typically have 1.5 mA critical current and 100 mΩ resistance, giving a 150 µV characteristic voltage and typical operating frequencies around 70 GHz. The insulating barriers for these junctions have significantly larger capacitance as compared to the negligible capacitance of SNS junctions, so that the SINIS junctions are critically damped with a unity McCumber parameter ($\beta c \approx 1$) and have nonhysteretic intrinsically stable IV curves. The first 1 V SINIS PJVS circuits contained 8192 junctions in a binary-array configuration of 14 bits [73,74]. An improved design was developed in 2002 [75]. The least significant bit consists of a single junction giving a resolution of 150 µV for the entire
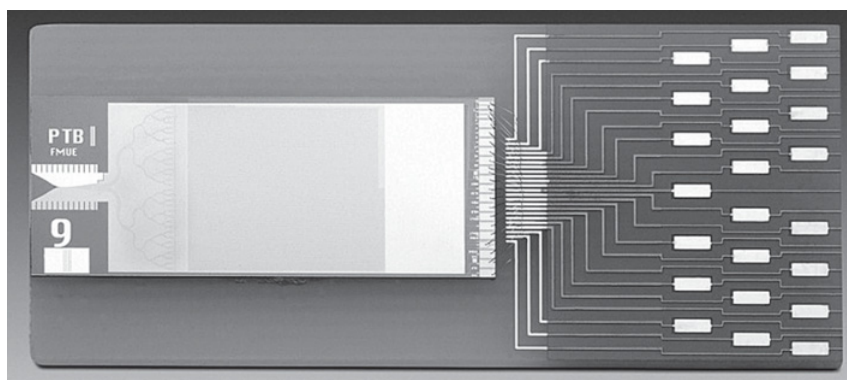
Fig. 13. Photograph of a 10 V PTB SINIS chip with 69,632 junctions and an operating current range of 0.6 mA. The chip is mounted on a chip carrier and its right edge is wire bonded to the breakout wiring pads. The finline launch for applying microwave bias can be seen on the left side (photographs courtesy of J. Kohlmann and F. Müller, PTB, 2007).

array. The first precision measurement performed was a comparison with a traditional array and had an operating current range of $200 \, \mu A$ [73]. Good agreement with the SIS array was found at 1 V with a measurement uncertainty of 2×10^{-10}. The first 10 V SINIS PJVS circuit consisted of 69,120 junctions integrated in 64 parallel branches with 1080 junctions each and operated over a current range of $200 \, \mu A$ [76,77]. Figure 13 shows a photograph of one of the most recent PTB 10 V PJVS circuits, which had a three-fold increase in current bias range of 0.6 mA [78,79].

As mentioned previously, the first realization of a PJVS circuit used externally shunted junctions [51]. Researchers in Finland have demonstrated frequency-dependent damping in a complex design with externally shunted junctions. The advantage of this technique is that higher-order steps can be stabilized, so that fewer junctions are needed for the same output voltage and bias frequency. For example, by operating the junctions on the $n = 3$ Shapiro step, their circuit that was biased at 70 GHz successfully produced 1 V output voltage with only 2310 junctions [80,81]. However, this design has not been attempted by other researchers, because operating margins have yet to be carefully investigated and because of the complexity of the externally shunted junctions.

Since stable voltages and fast programmability are much easier to achieve with PJVS systems, as compared with conventional JVS systems, these systems were quickly applied in many different areas that required high-precision voltage calibration: DVM linearity measurements [59,60], Zener standard calibrations [60], fast-reversed dc measurements of thermal converters [82,83], potentiometric systems [84], quantum voltmeters [85], watt balance experiments [12,52,53], and metrological triangle experiments [54]. A particularly important application was the direct implementation of a PJVS system into the NIST voltage dissemination chain, which eliminated the electrochemical cell artifact standards that were predominantly used in the last century [86].

Originally, the PJVS circuits were developed for synthesizing stepwise-approximated waveforms with a calculable rms value [51]. Figure 14(a) shows an idealized stepwise waveform with 16 samples and 2 V peak amplitude. Unfortunately, it was realized that the transients occurring during the switching of the bias electronics dramatically limit the voltage accuracy, especially for audio frequencies that were of primary interest. Even though the voltage steps are accurate, the voltage that is produced during step transitions is subject to both array characteristics and circuit details. The transitions therefore introduce errors in the rms voltage, especially for higher-frequency waveforms. More recently, the rise time of the bias electronics was reduced from a few microseconds [87] to around 200 ns [88], which allowed this PJVS waveform synthesis technique to be implemented for subkilohertz frequencies, particularly for power applications at (50–60) Hz [55,56,88–91].

In addition to the rise-time-related errors, the rms voltage is also affected by harmonics that are produced by the digital nature of the waveform, as shown in Fig. 14(b); for example, to ensure that the combined error of such digitization harmonics are less than $1 \, \mu V/V$, a 60 Hz
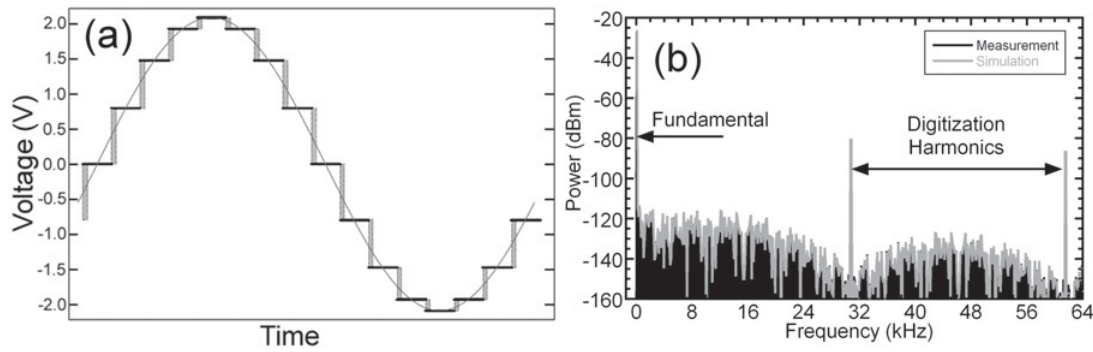
Fig. 14. (a) Idealized stepwise-approximated sine wave synthesized by the PJVS with a 2.1 V zero-to-peak amplitude and only 16 samples, showing perfectly quantized voltages and finite-width transitions between them. (b) Spectral measurement of a 512 sample 60 Hz sine wave generated by a Josephson array with 2.1 V amplitude zero-to-peak (1.5 V rms). Measured harmonics from the Josephson array (black) are in excellent agreement with the numerical simulations (the gray simulation curve exactly covers the black measured data). The first two most-significant pairs of digitization harmonics are shown near 32 kHz and 64 kHz.

waveform must have at least 1024 voltages [56]. The rms voltage accuracy of PJVS synthesized waveforms has been investigated with thermal voltage converters and transfer standards that integrate the entire waveform. As expected, the result has been shown to depend on the transition rise time [56,90,91]. Timing and bias variations produce systematic errors that also reduce the absolute rms voltage accuracy. Fortunately, these latter errors can be bounded, so that an rms voltage accuracy of a few parts in 10^7 can be achieved at very low frequencies, such as the (50–60) Hz waveforms that are of primary interest for power applications.

Analog-to-digital converters and sampling voltmeters are also particularly interesting instruments whose performance can be investigated with PJVS waveforms [89,92–94]. For these instruments, samples acquired in the transient regions can be discarded and those of the quantum-accurate voltage steps can be retained. Such measurements with integrating sampling voltmeters have been implemented in systems for ac power calibrations, and both direct and differential sampling techniques have been investigated. The accuracy and uncertainty of these methods are determined primarily by details of the measurement technique and performance of the sampler. While investigating the differential sampling technique, PTB researchers found that the synthesized waveforms from two PJVS systems agreed to better than 5 parts in 10^8 for stepwise-approximated sine waves with frequencies below 400 Hz [92]. These results were confirmed by NIST researchers who found an agreement better than 1 part in 10^8 (of the reconstructed rms amplitude) for 60 Hz, 64-state, stepwise-approximated sine waves [94]. Research of sampling measurement techniques with PJVS synthesized waveforms continues, because present results suggest that an uncertainty of a few parts in 10^7 can be achieved for measurements of an independent reference sine wave of high spectral purity and stability.

The performance of PJVS systems is continuing to improve. The amplitude of synthesized waveforms are being increased to 10 V, operating margins are approaching 1 mA, and more-accurate bias sources are being implemented that will expand the useful operating frequency range. In spite of their greater complexity, 10 V PJVS systems may eventually replace the conventional JVS for dc applications, because they provide the additional features of stable and fast programmable voltages and are more easily automated. The impact of PJVS waveform synthesis on precision ac measurements depends primarily upon understanding and improving the measurement techniques and instrumentation required for specific applications.

3.4.2 Pulse driven arrays

As mentioned in the previous section, the primary limitation of PJVS-synthesized waveforms is the inaccuracy that results from transitions between the quantized voltages. In 1996, a

different approach based on pulse-driven arrays provided a solution to this problem and a means to produce quantum-accurate voltage waveforms [57,95–97]. The operating principle is based on the use of a Josephson junction as a pulse quantizer, since the time integral of the voltage across the junction is quantized in multiples of the flux quantum $\phi_o = h/2e = K_{\mathrm{J}}^{-1}$. When a Josephson junction is biased with a current pulse of the proper amplitude and duration, then the junction will make exactly one perfectly quantized voltage pulse. If the pulse polarity is reversed, then the array can generate both positive and negative voltages [97].

A number of pulse-driven programmable voltage sources based on this idea are presently in use or under development for various applications [95–122]. Although they all create accurate waveforms with quantized pulses, various names have been used to emphasize their different features for different applications, such as the Josephson digital-to-analog converter for ac and dc voltages, the Josephson arbitrary waveform synthesizer (JAWS) emphasizing multiple-harmonic waveforms, the ac Josephson voltage standard (ACJVS) focusing on ac metrology for audio-frequency sine-wave synthesis, and the quantum voltage noise source (QVNS) for low-voltage applications such as noise thermometry [119–122].

To explain the operating principle of pulse-driven arrays, we first describe the method for synthesizing unipolar waveforms with pulses of a single polarity. This method is currently used for the low-voltage noise thermometry application. A single large array of N junctions is distributed along a wide-bandwidth transmission line and current biased with a pulse train at frequency f. If the bias conditions are properly set so that each junction generates exactly one quantized voltage pulse for every input pulse, then the array generates a pulse train with a time-averaged voltage Nf/K_{J} that is proportional to the pulse frequency. A unipolar (with amplitude range of 0 to Nf/K_{J}) output waveform can be generated by defining the presence (1) or absence (0) of pulses with a digital code generator. For example, using a clock frequency of $f_s = 10$ GHz, the 10-bit repeating pulse sequence 1111100000111110000. . . creates a square wave of amplitude of Nf_s/K_{J} at a frequency of 1 GHz. Unfortunately, such unipolar waveforms have an inherent dc component that is undesirable for many applications. Two methods were developed, which will be described below, that produce bipolar drive signals by combining a two-level digital code generator signal with an additional microwave signal [97,99]. Recently, a bipolar three-level pulse generator has become commercially available and was specifically designed for Josephson applications [114,118].

Figure 15 shows (b) a block diagram and (a, c) relevant waveforms of the process that are used to generate an accurate bipolar sine wave of frequency f_1 or any other periodic waveform from quantized Josephson pulses [97]. First, the desired analog voltage signal $S(t)$ is digitized as a periodic digital waveform (code) $S(i)$ that is calculated with a modulator algorithm, a computer program that digitizes the signal at a sampling frequency f_s. The algorithm is typically a first-order delta-sigma modulator that reduces the digitization harmonics for low frequencies. For periodic waveforms, the code is calculated and stored in the circulating memory of a digital code generator. When the digital code generator is clocked at the sampling frequency, it creates a timed series of bipolar bias-current levels for which the low-frequency spectral components precisely reproduce the desired original signal, as shown in Fig. 15(a). The code generator biases the array with the bipolar sequence of current levels of amplitude $\pm I_D$. The array is simultaneously biased with a sinusoidal microwave current I_{mw} of frequency $f = mf_s/2$ that is synchronized with the digital signal, where m is an integer greater than or equal to 2 (typically $m = 3$). This combined broadband bias signal produces bipolar current pulses. The resulting output Josephson waveform consists of bipolar voltage pulses that correspond to the digital waveform and are perfectly quantized. A low-pass filter can be used to remove the high-frequency digitization harmonics, which are typically significant only for frequencies above 10 MHz. The spectrum and the voltage of the output signal $S'(t)$ is precisely and accurately known as a result of the quantized pulses, and knowledge of the digital code, the sampling frequency, and the number of junctions in the array.

The above bias method was developed in order to generate a bipolar pulse drive with a two-level code generator. A more straightforward method would be to directly synthesize bipolar pulses with a three-level code generator. Such an instrument, which can produce three states, zero and pulses of both polarities, has been constructed [114], and has the potential to
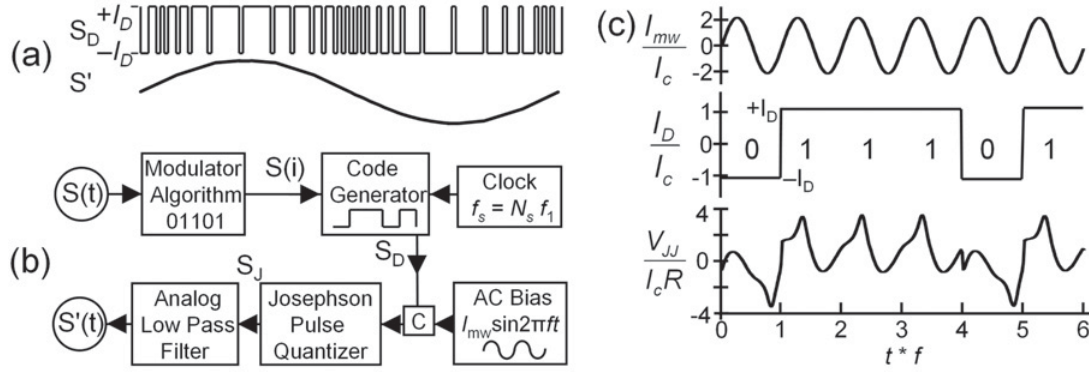
Fig. 15. Operating principle of the bipolar bias technique [97]. (a) Two-level bipolar digital signal S_D and its corresponding analog audio-frequency Josephson-quantized output signal S'. (b) Block diagram showing the main components and the various digital and analog signals. C is a directional coupler. (c) Input and output waveforms: the sinusoidal (microwave) current drive of amplitude I_{mw} at frequency $f = f_s$ ($m = 2$); digital current levels clocked at f_s; and the resulting bipolar quantized voltage pulses appearing across the junction pulse quantizer.

dramatically simplify the ACJVS system. Research is continuing to improve the performance of this bipolar pulse generator so that practical output voltages and operating margins can be demonstrated for ac waveforms [118].

Increasing the output voltage of the ACJVS synthesized waveforms has been a challenging task, and parallels the improvements described for the PJVS, such as the use of stacked Josephson junctions [22,62–67,101,110]. However, achieving higher voltage ACJVS circuits is additionally limited and complicated by the broadband nature of the digital bias signals. Different microwave components, especially on-chip filters [58,106], had to be developed to optimize the array performance for the broadband signals, and new techniques, such as the ac coupling technique [99], were required in order to combine the output signals of multiple arrays. The original unipolar design of the pulse-driven Josephson source was able to generate voltages of a few millivolts [57,58,95]. Implementation of the bipolar bias technique [97] increased the output voltage by a factor of six over the unipolar bias technique (for the same digital clock speed and $m = 3$). The ac coupling technique [99] allowed a further doubling of the output voltage by taking advantage of the dual complementary digital output channels of digital code generators.

Figure 16 shows the basic circuit schematic and chip layout for two arrays biased with the ac coupling technique. A simplified circuit schematic for the ac-coupling technique is shown in Fig. 16(a). Commercial bitstream generators typically have a second complementary data output (D−) that produces a bit sequence that is the ones-complement of the data output (D+), which for our purpose produces an analog waveform of inverted polarity. DC blocking capacitors (acting as broadband high-pass filters) remove the low-speed (in this case audio frequency) component of the digital bias signal. This prevents common-mode signals from appearing on the microwave terminations (not shown) and allows the low-speed, inductively filtered, output-voltage leads to float so that the two arrays can be connected in series. However, in order to achieve operating margins, the audio frequency bias (of appropriate polarity, $\pm I$) must be reapplied across each array. This "compensation" bias is provided through floating differential amplifiers and commercial arbitrary waveform generators with adjustable gain that are synchronized with the digital waveform. All of these biases must be synchronized and properly adjusted to ensure pulse quantization [22,95,99–105,111,115,116]. The ranges, over which the biases produce quantized pulses, are optimized and define the operating margins of the circuit. By using this bias technique and taking advantage of further improvements in microwave design and stacked junction fabrication [67], dual-array ACJVS circuits can presently generate rms amplitudes up to 275 mV (nearly 400 mV peak) [117].

Figure 17 shows a measurement of an ACJVS sine wave with the largest currently achievable rms output voltage, 275 mV [117]. The two series-connected arrays are biased with a 15 GHz
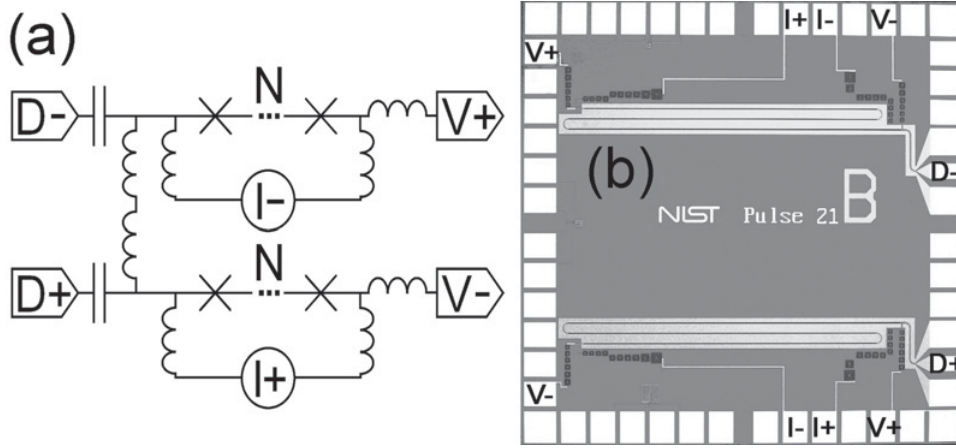
Fig. 16. Dual-array 275 mV rms ACJVS (a) circuit schematic and (b) photograph of the 1 cm × 1 cm chip, showing the relevant circuit and biases for the ac coupling technique, including the high-speed biases D, low-speed compensation biases I, and differential output voltage tapes V for each array. Also indicated in the schematic are the capacitive dc blocks, compensation current I, inductive low-pass filters, and N number of series junctions per array. Each array of 6400 double-stacked Josephson junctions is distributed along three parallel coplanar waveguide sections. The two voltage leads that are on the right side of the photograph (V+ (bottom array) and V− (top array)) are connected together to combine the two output voltage signals in series, as shown in the schematic.
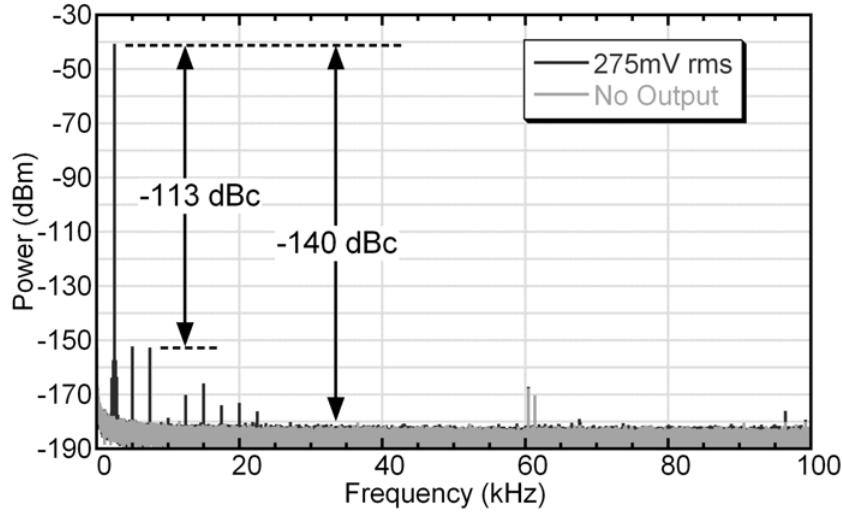

Fig. 17. Digitally sampled spectral measurement of the 275 mV, 2.5 kHz ACJVS sine wave. The digitizer used 1 MΩ input impedance, 10 V input range, 2 Hz resolution bandwidth, 10 averages, and a 500 kS/s sampling rate. Grey shaded data show the digitizer noise floor and spurious signals with the ACJVS pulses off. The −113 dBc measured distortion is produced by the digitizer's nonlinearities.

microwave drive and a 4 Mbit digital pattern clocked at 10 Gbit/s. With this bias configuration, waveforms can be synthesized with a minimum frequency of 2.5 kHz. The measured spectrum shows an accurate sine wave with no measurable distortion to the −140 dBc [dB below the fundamental (carrier)] noise floor of the measurement. The harmonics observed between 5 kHz and 22.5 kHz are extremely low (amplitudes < −113 dBc) and are produced by small nonlinearities of the measurement instrument [98,102,111,117].

After ten years of research and development, the first practical ACJVS system was implemented in 2006 as a dual-array circuit that was capable of producing 100 mV rms [108,109].
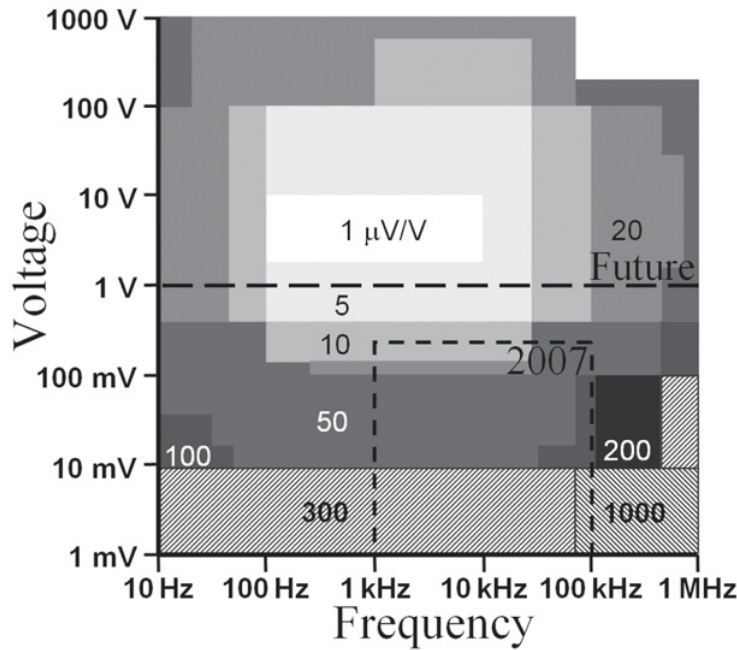
Fig. 18. Voltage vs. frequency plot showing the uncertainty boundaries (in units of μV/V) for ac voltage calibrations at NIST (courtesy of T. Lipe and J. Kinard, NIST). Dash-delimited regions indicate current (2007) and "future" (below the long dashed line) parameter ranges impacted by the ACJVS quantum-based voltage source.

It was designed to characterize thermal converters and transfer standards whose rms comparison technique of the ac-dc difference voltages is the dominant method used to perform ac voltage calibrations. It was formally implemented in the NIST calibration service, and reduced the ac voltage calibration uncertainty by as much as an order of magnitude over traditional ac-dc transfer methods [113]. Figure 18 shows the ac calibration uncertainty offered by NIST as a function of frequency and voltage. These uncertainties are based on a range of calibration techniques, but primarily on rms detection. The region of present impact for the current 275 mV rms ACJVS quantum-based voltage source is the dashed "2007" box that covers the frequency range from 1 kHz to 100 kHz. Future goals for ACJVS development are to expand the frequency range up to 1 MHz [115,116] and to quadruple the rms output voltage to 1 V by use of the ac-coupled bias technique and eight arrays connected in series [117]. There is enough room on a 1 cm square chip for eight arrays. The challenge is to simultaneously create and synchronize the output waveforms of the eight broadband and compensation bias signals. Implementation of this approach is currently limited by the unavailability of high-speed code generators that can produce more than two synchronized digital waveforms.

It is expected that this newly developed ac Josephson voltage source will find many applications in metrology and precision measurements. As mentioned earlier, a low-voltage version of the pulse-driven source, called the quantized voltage noise source (QVNS), is being used in an electronic primary thermometer that is based on measurements of Johnson noise in a resistor [119–122]. In these experiments, the QVNS produces a calculable pseudo-noise waveform with a comb of random-phase harmonics each having identical voltage amplitude. The synthesized arbitrary waveform is used to calibrate the non linearity and gain of the cross-correlation electronics that are used to measure the voltage noise of the resistor, and therefore its temperature. The quantum-based Johnson noise thermometry system has been used to measure the ratio of the triple-point temperatures of gallium and water to within an accuracy better than 100 μK/K [121]. The system has also provided useful measurements of the deviations of the International Temperature Scale of 1990 (ITS-90) from thermodynamic temperature at the moderately high temperatures of the zinc (692.677 K) and tin (505.078 K) freezing points [122].

With further improvements and reduction in systematic errors, the noise thermometry system may contribute to the redefinition of Boltzmann's constant, because it offers an electronic approach that is distinctly different from the various gas-thermometry and other approaches that have been previously pursued.

Lastly, a couple of unique approaches should be mentioned that may be able to produce accurate quantum-based ac voltage waveforms that also control single quantized voltage pulses and take advantage of more than a decade of extensive research and development of superconducting digital electronics [123–125]. A number of voltage-multiplier circuits have been designed and tested that allow a single pulse from a Josephson junction to propagate through a circuit and trigger pulses in other junctions in such a way that the output voltage is multiplied. Some designs use a number of cascaded multiplier stages, while other designs use different types of on-chip superconducting circuits for signal amplification. One advantage of these designs is that they operate at relatively low-speed, especially the input stages, because higher voltages are produced with multiplier stages. They also may be able to generate rf arbitrary waveforms with low distortion at frequencies higher than are currently possible with the ACJVS approach. The disadvantages of these circuits are that they are far more complex than simple pulse-driven distributed arrays and it has been difficult to demonstrate experimental circuits that have useful bias margins and voltages larger than 50 mV.

4 Conclusions

Over the past 30 years, the Josephson effect has enabled the development of unique electrical devices and systems, including SQUIDs, detectors, analog-to-digital converters, and, most importantly for electrical metrology, voltage standards. The greatest impact that the Josephson effect has had in electrical metrology, has been to clearly demonstrate that intrinsically accurate quantum-based standards provide unprecedented performance as compared with artifact standards, whose values depend on the environmental conditions and time. A similar revolution took place in resistance metrology with the discovery of the quantum Hall effect. Since 1990, the two quantum effects allow the representation of the electrical units volt and ohm based on fundamental constants. There is overwhelming experimental evidence that the Josephson voltage and the quantized Hall resistance are universal quantities. These electrical quantum effects are used world-wide as invariant references in electrical calibrations and have improved the reproducibility of calibration results by up to two orders of magnitude during the last two decades.

Nowadays, more than 60 conventional Josephson voltage standards are routinely used around the world for dc metrology applications. Programmable Josephson voltage standards are also in operation for dc calibrations and are currently being implemented in low-frequency (< 400 Hz) ac applications, in particular for the calibration of ac power instruments. They are also parts of more complex precision experiments such as the Watt balances. Pulse-driven ac Josephson voltage standards are currently in development in seven metrology laboratories for applications in ac metrology at frequencies up to a few hundred kilohertz and at rms voltages up to 275 mV. This ACJVS has already been used to reduce the measurement uncertainties of thermal transfer standards and to measure and characterize the nonlinearities and the low harmonic distortion of high-performance digitizers. The quantized voltage noise source, a low voltage version of the ACJVS, has already played an important role in understanding the ITS-90 temperature scale and has the potential to provide an electronic temperature standard that may impact the redefinition of the Boltzmann constant. Furthermore, many other novel applications of these systems can be anticipated because the accuracy and the stability provided by their quantum-nature can be exploited for a vast range of precision measurements and used for enhancing the behaviour of other high-performance devices. Future research will likely focus on extending these performances to a wider parameter space than that shown in Fig. 18, such as to higher voltages and higher frequencies.

In addition to the huge improvement brought by the Josephson and the quantum Hall effects in electrical calibration, the two quantum effects will also play a major role in the next

modernization of the SI. In the long term, the definition of the conventional values $K_{\text{J-90}}$ and $R_{\text{K-90}}$ is unsatisfactory because the consistency of the SI system as a whole still depends on difficult experiments that link mechanical and electrical units. Moreover, the unit of mass, which is one of the base mechanical units, is the last remaining artefact in the SI. The kilogram is defined as the mass of the international prototype of the kilogram, made of platinum-iridium and kept at the BIPM under special conditions. One of the major disadvantages of this definition is the fact that the kilogram is subject to possible changes in time. As a consequence, the electrical units, which all depend on the kilogram, may also drift with time. Extraordinary efforts are underway to find a proper replacement of the present kilogram definition based on fundamental constants (see [126] for a review).

Recently, new definitions have been proposed for the kilogram, ampere, kelvin and mole so that the units are linked to fixed values of fundamental constants [127]. In this new SI, the kilogram would be defined in terms of the Planck constant h and the ampere in terms of the elementary charge e. As a consequence, the Josephson constant and the von Klitzing constant would become exactly known, thereby allowing the Josephson and quantum Hall effects to be direct realizations of the electrical SI units with no uncertainty contribution from the uncertainty of K_{J} and/or R_{K}.

References

1. B.D. Josephson, Phys. Lett. **1**, 251 (1962)
2. S. Shapiro, Phys. Rev. Lett. **11**, 80 (1963)
3. B. Jeckelmann, B. Jeanneret, Rep. Prog. Phys. **64**, 1603 (2001)
4. A.M. Thompson, D.G. Lampard, Nature (London) **177**, 888 (1956)
5. A. Hartland, R. Jones, B. Kibble, D. Legg, IEEE Trans. Instrum. Meas. **36**, 208 (1987)
6. A. Jeffery, R. Elmquist, L. Lee, J. Shields, R. Dziuba, IEEE Trans. Instrum. Meas. **46**, 264 (1997)
7. G. Small, B. Rickets, P. Coogan, B. Pritchard, M. Sovierzoski, Metrologia **34**, 241 (1997)
8. P.J. Mohr, B.N. Taylor, D.B. Newell, Rev. Mod. Phys. **80**, 633 (2008)
9. R.S. van Dyck, P.B. Schwinberg, H.G. Dehmelt, *The Electron* (Kluwer Academic, The Netherlands, 1991), pp. 239–293
10. T. Kinoshita, Rep. Prog. Phys. **59**, 1459 (1996)
11. A. Eichenberger, B. Jeckelmann, P. Richard, Metrologia **40**, 356 (2003)
12. R.L. Steiner, E.R. Williams, R. Liu, D. Newel, IEEE Trans. Instrum. Meas. **56**, 592 (2007)
13. B.N. Taylor, T.J. Witt, Metrologia **26**, 47 (1989)
14. B.P. Kibble, I.A. Robinson, J.H. Belliss, Metrologia **27**, 173 (1990)
15. C.A. Hamilton, C.J. Burroughs, K. Chieh, J. Res. Nat. Inst. Stand. Technol. **95**, 219 (1990)
16. R.L. Kautz, *Metrology at the Frontier of Physics and Technology*, edited by L. Crovini, T.J. Quinn (North-Holland, Amsterdam, 1992), pp. 259–296
17. R. Pöpel, Metrologia **29**, 153 (1992)
18. J. Niemeyer, *Handbook of Appl. Supercond.*, Vol 2: Applications (IOP, Bristol, 1998), pp. 1813–1834
19. C.A. Hamilton, Rev. Sci. Instrum. **71**, 3611 (2000)
20. R. Behr, F. Müller, J. Kohlmann, *Studies of Josephson Junction Arrays II: Studies of High Temperature Superconductors*, edited by A.V. Narlikar (Huntington, Nova Science Publ., 40, 2002), pp. 155–184
21. J. Kohlmann, R. Behr, T. Funk, Meas. Sci. Technol. **14**, 1216 (2003)
22. S.P. Benz, C. Hamilton, Proc. IEEE **92**, 1617 (2004)
23. W.C. Stewart, Appl. Phys. Lett. **12**, 277 (1968)
24. D.E. McCumber, J. Appl. Phys. **39**, 3113 (1968)
25. R.L. Kautz, Rep. Progr. Phys. **59**, 935 (1996)
26. J.S. Tsai, A.K. Jain, J.E. Lukens, Phys. Rev. Lett. **51**, 316 (1983)

27. J. Niemeyer, L. Grimm, C.A. Hamilton, R.L. Steiner, IEEE Electron Device Lett. **EDL7**, 44 (1986)
28. A.K. Jain, J.E. Lukens, J.S. Tsai, Phys. Rev. Lett. **58**, 1165 (1987)
29. R.L. Kautz, F.L. Lloyd, Appl. Phys. Lett. **51**, 2043 (1987)
30. I.Y. Krasnopolin, R. Behr, J. Niemeyer, Supercond. Sci. Technol. **15**, 1034 (2002)
31. J. Clarke, Phys. Rev. Lett. **21**, 1566 (1968)
32. D.G. McDonald, Phys. Today 46 (2001)
33. T. Endo, M. Koyanagi, A. Nakamura, IEEE Trans. Instrum. Meas. **IM-32**, 267 (1983)
34. M.T. Levinsen, R.Y. Chiao, M.J. Feldman, B.A. Tucker, Appl. Phys. Lett. **31**, 776 (1977)
35. J. Niemeyer, J.H. Hinken, R.L. Kautz, Appl. Phys. Lett. **45**, 478 (1984)
36. C.A. Hamilton, R.L. Kautz, R.L. Steiner, F. Lloyd, IEEE Electron Device Lett. **EDL-6**, 623 (1985)
37. J. Niemeyer, L. Grimm, W. Meier, J.H. Hinken, E. Vollmer, Appl. Phys. Lett. **47**, 1222 (1985)
38. F. Lloyd, C.A. Hamilton, J. Beall, D. Go, R.H. Ono, R.E. Harris, IEEE Electron Device Lett. **EDL-8**, 449 (1987)
39. D. Reymann, T.J. Witt, G. Eklund, H. Pajander, H. Nilsson, R. Behr, T. Funk, F. Müller, IEEE Trans. Instrum. Meas. **48**, 257 (1999)
40. C.A. Hamilton, Y.H. Tang, Metrologia **36**, 53 (1999)
41. T.J. Witt, IEE Proc.-Sci. Meas. Technol. **149**, 305 (2002)
42. T.J. Witt, IEEE Trans. Instrum. Meas. **46**, 318 (1997)
43. T.J. Witt, D. Reymann, IEE Proc.-Sci. Meas. Technol. **147**, 177 (2000)
44. C.M. Wang, C.A. Hamilton, Metrologia **35**, 33 (1998)
45. D. Reymann, T.J. Witt, P. Vrabcek, Y. Tang, C.A. Hamilton, A.S. Katkov, B. Jeanneret, O. Power, IEEE Trans. Instrum. Meas. **50**, 206 (2001)
46. J.I. Giem, IEEE Trans. Instrum. Meas. **40**, 329 (1991)
47. S.P. Benz, Appl. Phys. Lett. **67**, 2714 (1995)
48. H. Sachse, R. Pöpel, T. Weimann, F. Müller, G. Hein, J. Niemeyer, Inst. Phys. Conf. Ser. **158**, 555 (1997)
49. H. Schulze, R. Behr, F. Müller, J. Niemeyer, Appl. Phys. Lett. **73**, 996 (1998)
50. H. Yamamori, M. Itoh, H. Sasaki, A. Shoji, S.P. Benz, P.D. Dresselhaus, Supercond. Sci. Technol. **14**, 1048 (2001)
51. C.A. Hamilton, C.J. Burroughs, R. Kautz, IEEE Trans. Instrum. Meas. 44, 223 (1995)
52. R.L. Steiner, D.B. Newell, E.R. Williams, R. Liu, P. Gournay, IEEE Trans. Instrum. Meas. **54**, 846 (2005)
53. W. Beer, A.L. Eichenberger, B. Jeanneret, B. Jeckelmann, A.R. Pourzand, P. Richard, J.P. Schwarz, IEEE Trans. Instrum. Meas. **52**, 62 (2003)
54. F. Piquemal, G. Genevès, Metrologia **37**, 207 (2000)
55. R. Behr, L. Palafox, J. Schurr, J. Williams, J. Melcher, in *Proc. of the 6th International Seminar in Electrical Metrology*, September 21-23 (2005), Rio de Janeiro, Brazil, pp. 11–12
56. C.J. Burroughs, S.P. Benz, P.D. Dresselhaus, B.C. Waltrip, T.L. Nelson, Y. Chong, J.M. Williams, D. Henderson, P. Patel, L. Palafox, R. Behr, IEEE Trans. Instrum. Meas. **56**, 289 (2007)
57. S.P. Benz, C.A. Hamilton, Appl. Phys. Lett. **68**, 3171 (1996)
58. S.P. Benz, C.A. Hamilton, C.J. Burroughs, T. Harvey, L.A. Christian, J. Przybysz, IEEE Trans. Appl. Supercond. **8**, 42 (1998)
59. S.P. Benz, C.A. Hamilton, C.J. Burroughs, T.E. Harvey, L.A. Christian, Appl. Phys. Lett. **71**, 1866 (1997)
60. B. Jeanneret, A. Rüfenacht, C.J. Burroughs, IEEE Trans. Instrum. Meas. **50**, 188 (2001)
61. J. Lo-Hive, S. Djordjevic, P. Cancela, F. Piquemal, R. Behr, C. Burroughs, H. Seppä, IEEE Trans. Instrum. Meas. **52**, 516 (2003)
62. Y. Chong, P. Dresselhaus, S. Benz, Appl. Phys. Lett. **86**, 2505 (2005)
63. Y. Chong, C. Burroughs, P. Dresselhaus, N. Hadacek, H. Yamamori, S. Benz, IEEE Trans. Instrum. Meas. **54**, 616 (2005)
64. Y. Chong, C. Burroughs, P. Dresselhaus, N. Hadacek, H. Yamamori, S. Benz, IEEE Trans. Appl. Supercond. **15**, 461 (2005)
65. C.J. Burroughs, S.P. Benz, P.D. Dresselhaus, Y. Chong, H. Yamamori, IEEE Trans. Appl. Supercond. **15**, 465 (2005)
66. B. Baek, P.D. Dresselhaus, S.P. Benz, IEEE Trans. Appl. Supercond. **16**, 1966 (2006)

67. P. Dresselhaus, S. Benz, C. Burroughs, N. Bergren, Y. Chong, IEEE Trans. Appl. Supercond. **17**, 173 (2007)
68. C. Urano, Y. Murayama, A. Iwasa, A. Shoji, H. Yamamori, M. Ishizaki, IEEE Trans. Instrum. Meas. **54**, 645 (2005)
69. M. Ishizaki, H. Yamamori, A. Shoji, P. Dresselhaus, S. Benz, IEEE Trans. Instrum. Meas. **54**, 620 (2005)
70. H. Yamamori, M. Ishizaki, A. Shoji, P. Dresselhaus, S. Benz, Appl. Phys. Lett. **88**, 2503 (2006)
71. H. Yamamori, M. Ishizaki, H. Sasaki, A. Shoji, IEEE Trans. Appl. Supercond. **17**, 858 (2007)
72. F. Müller, H. Schulze, R. Behr, J. Kohlmann, J. Niemeyer, Physica C **354**, 66 (2001)
73. R. Behr, H. Schulze, F. Müller, J. Kohlmann, J. Niemeyer, IEEE Trans. Instrum. Meas. **48**, 270 (1999)
74. H. Schulze, F. Müller, R. Behr, J. Kohlmann, J. Niemeyer, D. Balashov, IEEE Trans. Appl. Supercond. **9**, 4241 (1999)
75. O. Kieler, R. Behr, F. Müller, H. Schulze, J. Kohlmann, J. Niemeyer, Physica C **372-376**, 309 (2002)
76. H. Schulze, R. Behr, J. Kohlmann, J. Niemeyer, Supercond. Sci. Technol. **13**, 1293 (2000)
77. J. Kohlmann, H. Schulze, R. Behr, F. Müller, J. Niemeyer, IEEE Trans. Instrum. Meas. **50**, 192 (2001)
78. F. Müller, R. Behr, L. Palafox, J. Kohlmann, R. Wendisch, I. Krasnopolin, IEEE Trans. Appl. Supercond. **17**, 649 (2007)
79. J. Kohlmann, F. Müller, O. Kieler, R. Behr, L. Palafox, M. Kahmann, J. Niemeyer, IEEE Trans. Instrum. Meas. **56**, 472 (2007)
80. J. Hassel, H. Seppä, L. Grönberg, I. Suni, IEEE Trans. Instrum. Meas. **50**, 195 (2001)
81. J. Hassel, H. Seppä, L. Grönberg, I. Suni, Rev. Sci. Instrum. **74**, 3510 (2003)
82. C. Burroughs, S. Benz, C.A. Hamilton, T. Harvey, J.R. Kinard, T.E. Lipe, H. Sasaki, IEEE Trans. Instrum. Meas. **48**, 282 (1999)
83. T. Funck, R. Behr, M. Klonz, IEEE Trans. Instrum. Meas. **50**, 322 (2001)
84. R. Behr, T. Funck, B. Schumacher, P. Warnecke, IEEE Trans. Instrum. Meas. **52**, 521 (2003)
85. R. Behr, L. Grimm, T. Funck, J. Kohlmann, H. Schulze, F. Müller, B. Schumacher, P. Warnecke, J. Niemeyer, IEEE Trans. Instrum. Meas. **50**, 185 (2001)
86. J. Sims, Y. Tang, NCSLI Measure **1**, 42 (2006)
87. C.A. Hamilton, C.J. Burroughs, S.P. Benz, J.R. Kinard, IEEE Trans. Instrum. Meas. **46**, 224 (1997)
88. P. Kleinschmidt, P. Patel, J. Williams, T. Janssen, IEE Proc.-Sci. Meas. Technol. **149**, 313 (2002)
89. L. Palafox, G. Ramm, R. Behr, W.G.K. Ihlenfeld, H. Moser, IEEE Trans. Instrum. Meas. **56**, 534 (2007)
90. R. Behr, J. Williams, P. Patel, T. Janssen, T. Funck, M. Klonz, IEEE Trans. Instrum. Meas. **54**, 612 (2005)
91. C.J. Burroughs, A. Rüfenacht, S.P. Benz, P.D. Dresselhaus, B.C. Waltrip, T.L. Nelson, IEEE Trans. Inst. Meas. **57**, 1322 (2008)
92. R. Behr, L. Palafox, G. Ramm, H. Moser, J. Melcher, IEEE Trans. Instrum. Meas. **56**, 235 (2007)
93. W.G.K. Ihlenfeld, E. Mohns, R. Behr, J. Williams, P. Patel, G. Ramm, H. Bachmair, IEEE Trans. Instrum. Meas. **54**, 649 (2005)
94. A. Rüfenacht, C.J. Burroughs, S.P. Benz, Rev. Sci. Instrum. **79**, 044704 (2008)
95. S.P. Benz, C.J. Burroughs, C.A. Hamilton, IEEE Trans. Appl. Supercond. **7**, 2653 (1997)
96. C.A. Hamilton, C.J. Burroughs, S.P. Benz, IEEE Trans. Appl. Supercond. **7**, 3756 (1997)
97. S.P. Benz, C.A. Hamilton, C.J. Burroughs, T. Harvey, IEEE Trans. Instrum. Meas. **48**, 266 (1999)
98. S.P. Benz, C.J. Burroughs, P.D. Dresselhaus, Appl. Phys. Lett. **77**, 1014 (2000)
99. S.P. Benz, C.J. Burroughs, P.D. Dresselhaus, IEEE Trans. Appl. Supercond. **11**, 612 (2001)
100. S.P. Benz, C.J. Burroughs, P.D. Dresselhaus, L. Christian, IEEE Trans. Instrum. Meas. **50**, 181 (2001)
101. S.P. Benz, P.D. Dresselhaus, C.J. Burroughs, IEEE Trans. Instrum. Meas. **50**, 1513 (2001)
102. S.P. Benz, F.L. Walls, P.D. Dresselhaus, C.J. Burroughs, IEICE Trans. Electron. **E85-C**, 608 (2002)
103. C.J. Burroughs, S.P. Benz, P.D. Dresselhaus, IEEE Trans. Instrum. Meas. **52**, 542 (2003)
104. J. Williams, T. Janssen, L. Palafox, D. Humphreys, R. Behr, J. Kohlmann, F. Müller, Supercond. Sci. Technol. **17**, 815 (2004)

105. C.J. Burroughs, S.P. Benz, P.D. Dresselhaus, Y. Chong, IEEE Trans. Instrum. Meas. **54**, 624 (2005)
106. M. Watanabe, P.D. Dresselhaus, S.P. Benz, IEEE Trans. Appl. Supercond. **16**, 49 (2006)
107. N. Hadacek, P.D. Dresselhaus, S.P. Benz, IEEE Trans. Appl. Supercond. **16**, 2005 (2006)
108. S.P. Benz, C.J. Burroughs, P.D. Dresselhaus, T.E. Lipe, J.R. Kinard, in *2006 Conference on Precision Electromagnetic Measurements Digest*, 10-14 July (2006), Torino, Italy, pp. 678–679
109. S. Benz, C.J. Burroughs, P.D. Dresselhaus, N.F. Bergren, T.E. Lipe, J.R. Kinard, Y. Tang, IEEE Trans. Instrum. Meas. **56**, 239 (2007)
110. O. Kieler, J. Kohlmann, R. Behr, F. Müller, L. Palafox, J. Niemeyer, IEEE Trans. Appl. Supercond. **17**, 187 (2007)
111. S.P. Benz, P.D. Dresselhaus, C.J. Burroughs, N.F. Bergren, IEEE Trans. Appl. Supercond. **17**, 864 (2007)
112. O.F. Kieler, J. Kohlmann, F. Müller, Supercond. Sci. Technol. **20**, S318 (2007)
113. T.E. Lipe, J.R. Kinard, Y. Tang, S.P. Benz, C.J. Burrroughs, P.D. Dresselhaus, Metrologia **45**, 275 (2008)
114. H.E. van den Brom, E. Houtzager, B.E.R. Brinkmeier, O.A. Chevtchenko, IEEE Trans. Instrum. Meas. **57**, 428 (2008)
115. O.F. Kieler, R.P. Landim, S.P. Benz, P.D. Dresselhaus, C.J. Burroughs, IEEE Trans. Instrum. Meas. **57**, 791 (2008)
116. R.P. Landim, S.P. Benz, P.D. Dresselhaus, C.J. Burroughs, IEEE Trans. Instrum. Meas. **57**, 289 (2008)
117. S.P. Benz, P.D. Dresselhaus, N.F. Bergren, R.P. Landim, *Conference on Precision Electromagnetic Measurements Digest*, 9-13 June (2008), Broomfield, CO, pp. 48–49
118. E. Houtzager, S.P. Benz, H.E. van den Brom, *Conference on Precision Electromagnetic Measurements Digest*, 9-13 June (2008), Broomfield, CO, pp. 46–47
119. S.P. Benz, J. Martinis, P.D. Dresselhaus, S.N. And, IEEE Trans. Instrum. Meas. **52**, 545 (2003)
120. S. Nam, S.P. Benz, P.D. Dresselhaus, W. Tew, D. White, J. Martinis, IEEE Trans. Instrum. Meas. **52**, 550 (2003)
121. S. Nam, S.P. Benz, P.D. Dresselhaus, C.J. Burroughs, W. Tew, D. White, J. Martinis, IEEE Trans. Instrum. Meas. **54**, 653 (2005)
122. J.R. Labenski, W.L. Tew, S.P. Benz, S.W. Nam, P. Dresselhaus, *Proceedings of the 10th International Symposium on Temperature and Thermal Measurements in Industry and Science* (TEMPMEKO 2007), 21-25 May (2007), Lake Louise, Canada (VDE Verlag, Berlin, 2008) (to appear)
123. V.K. Semenov, IEEE Trans. Appl. Supercond. **3**, 2637 (1993)
124. Y. Mizugaki, Y. Namatame, M. Maezawa, Supercond. Sci. Technol. **20**, S315 (2007)
125. O. Mukhanov, A. Inamdar, T. Filippov, A. Sahu, S. Sarwana, V. Semenov, IEEE Trans. Appl. Supercond. **17**, 416 (2007)
126. W. Schwitz, B. Jeckelmann, P. Richard, C. R. Physique **5**, 881 (2004)
127. I.M. Mills, P.J. Mohr, T.J. Quinn, B.N. Taylor, E.R. Williams, Metrologia **43**, 227 (2006)